SIGGRAPH ASIA 2021 TOKYO LIVE

Differentiable Time-Gated Rendering

Lifan Wu[1]*, Guangyan Cai[2]*,
Ravi Ramamoorthi[3], and Shuang Zhao[2]

[1]NVIDIA
[2]University of California, Irvine
[3]University of California, San Diego
(* equal contribution)

Time-of-Flight Light Transport

- ToF Imaging

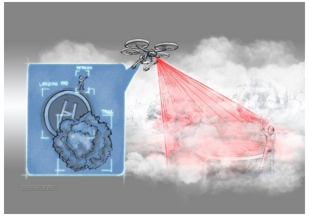

Seeing through fog
[Satat et al. 2018]

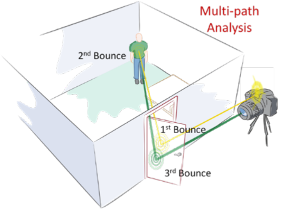

Looking around corners
[Velten et al. 2012]

- Time-Gated Forward rendering

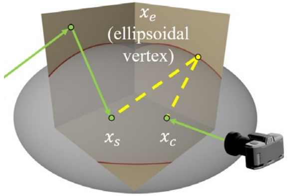

Ellipsoidal connections
[Pediredla et al. 2019]

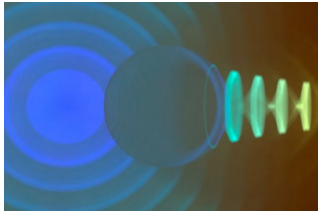

Transient rendering
[Jarabo et al. 2014]

Time-resolved measurements are useful

Consider lengths of light paths when sampling

Time-Gated Inverse Rendering

- Non-line-of-sight (NLOS) shape optimization based on **gradients**

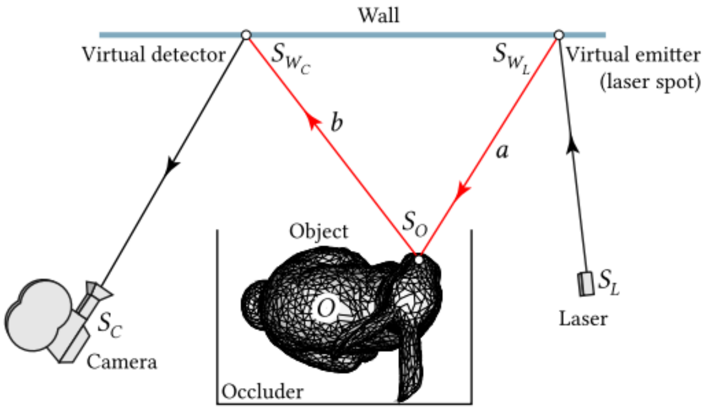

[Tsai et al. 2019]
[Iseringhausen and Hullin 2020]

Light transport limited to **3 bounces** (only one bounce on the unseen object)

Challenging to reconstruct **concave** shapes

Physics-Based Differentiable Rendering

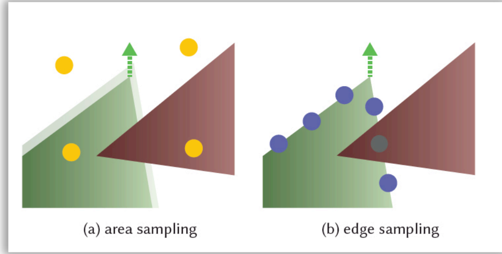

[Li et al. 2018]

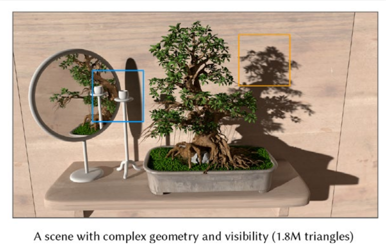

[Loubet et al. 2019]

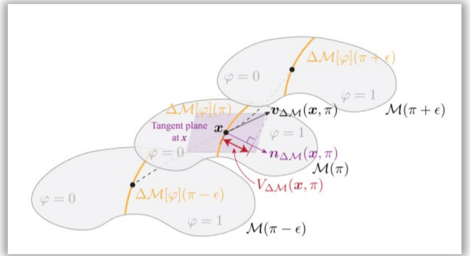

[Zhang et al. 2020]

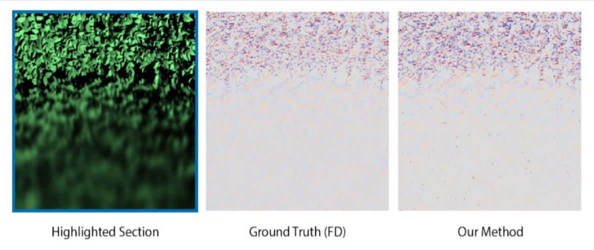

[Bangaru et al. 2020]

Complex light transport

Differentiating **arbitrary** scene parameters

Steady-state rendering only

Our Contributions

Forward rendering

ToF camera

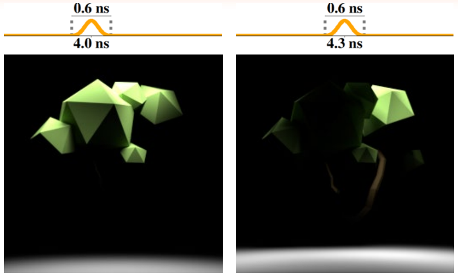

Time-gated rendering

Differentiation

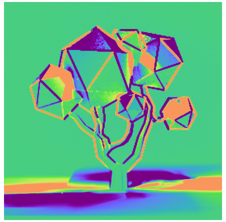

Steady-state differentiable rendering

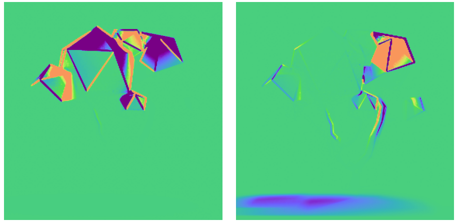

Differentiable time-gated rendering

Theoretical formulation

Monte Carlo estimators

Preview of Results

Time-Gated Derivatives

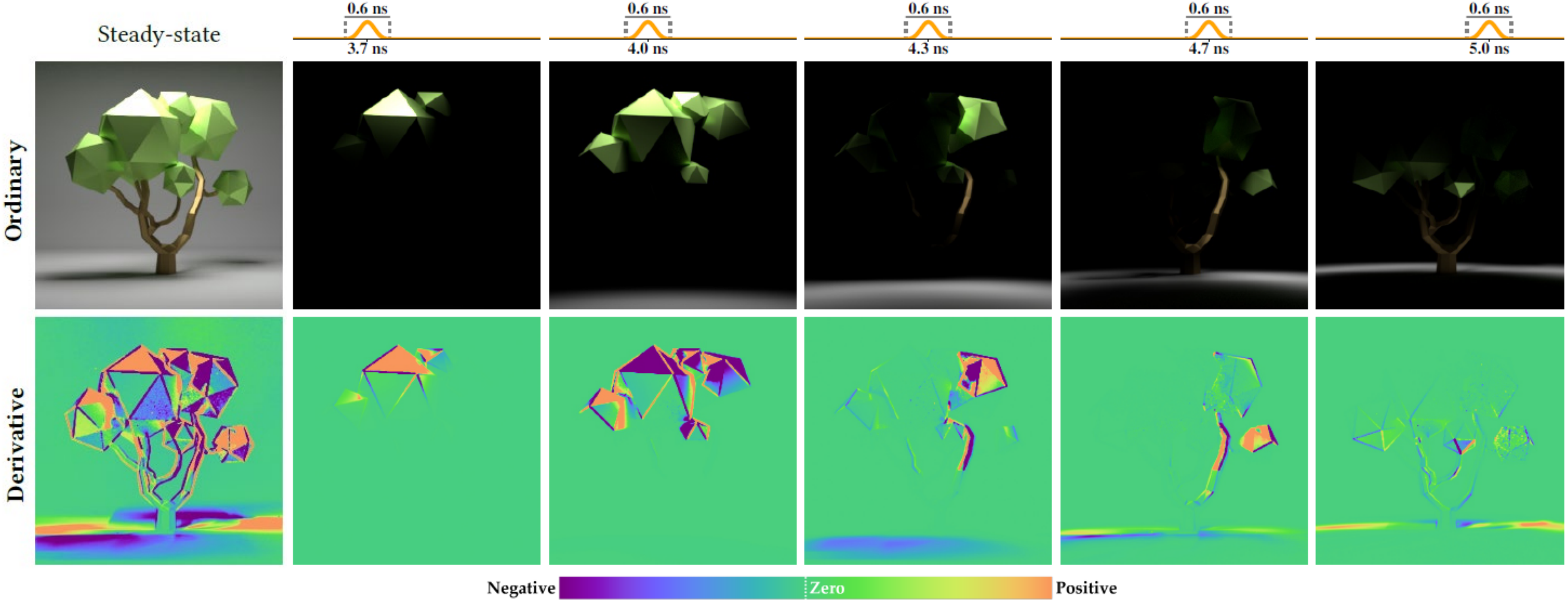

Preview of Results

Inverse Rendering

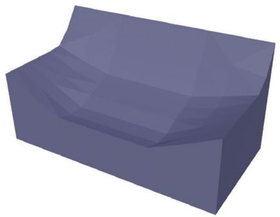

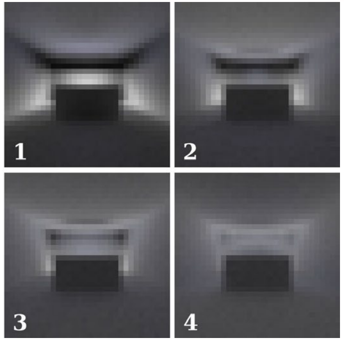

Target (20 ToF images used, 4 shown)

Optimized

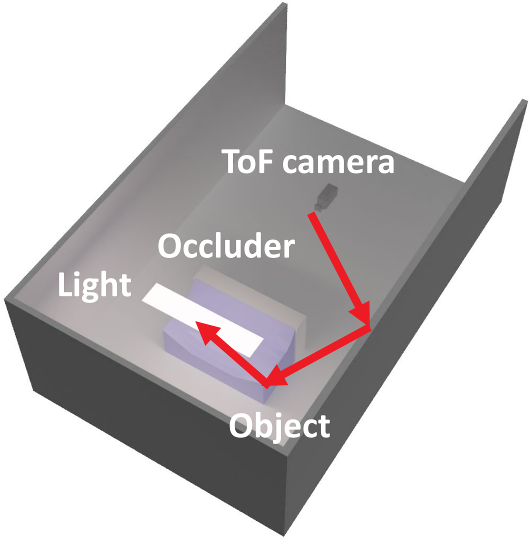

NLOS configuration
(59 unknown variables)

Differentiable Time-Gated Theory

Path Integral

$$I = \int_{\mathbf{\Omega}} f(\bar{\boldsymbol{x}})\,\mathrm{d}\mu(\bar{\boldsymbol{x}})$$

- Introduced by Veach [1997]
- Ω : Path space
- $f(\bar{\boldsymbol{x}})$: Measurement contribution function
- $\mathrm{d}\mu(\bar{\boldsymbol{x}})$: Area-product measure

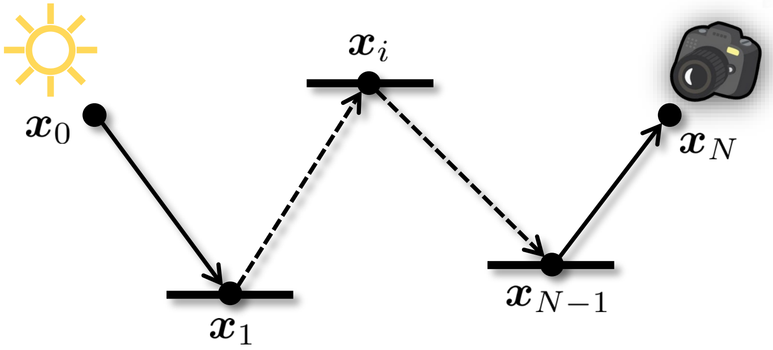

Light path $\bar{\boldsymbol{x}} = (\boldsymbol{x}_0, \ldots, \boldsymbol{x}_N)$

Time-Gated Path Integral

$$I = \int_{\Omega} \boxed{W_\tau(\|\bar{\boldsymbol{x}}\|)}\, f(\bar{\boldsymbol{x}})\,\mathrm{d}\mu(\bar{\boldsymbol{x}})$$

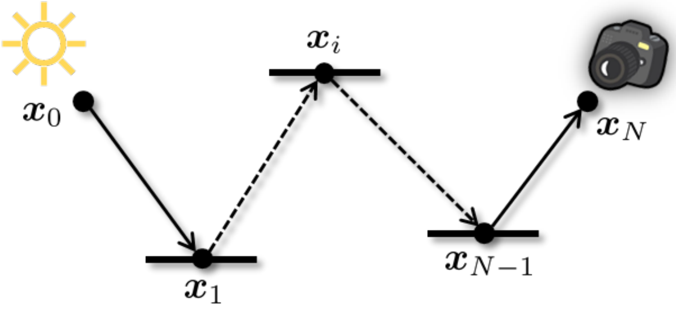

- Path-length importance function $W_\tau(\|\bar{\boldsymbol{x}}\|)$
- Path length $\|\bar{\boldsymbol{x}}\| = \sum_{i=1}^{N} \|\boldsymbol{x}_i - \boldsymbol{x}_{i-1}\|$

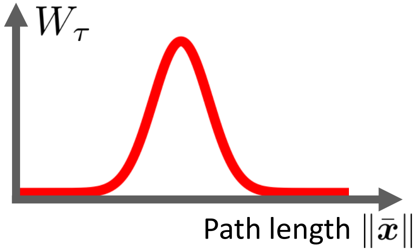

Gaussian

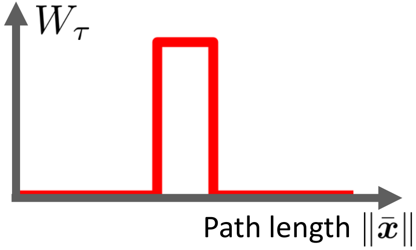

Boxcar

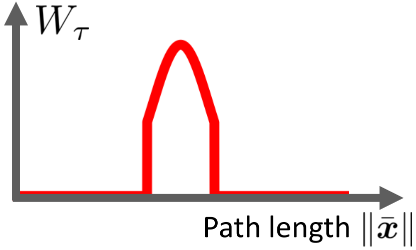

Truncated Gaussian

Material-Form Reparameterization

Time-gated path integral

$$I = \int_{\mathbf{\Omega}(\theta)} W_\tau(\|\bar{\boldsymbol{x}}\|)\, f(\bar{\boldsymbol{x}})\, \mathrm{d}\mu(\bar{\boldsymbol{x}})$$

Material-form time-gated path integral

$$I = \int_{\hat{\Omega}} W_\tau(\|\bar{\boldsymbol{x}}\|)\, \underbrace{f(\bar{\boldsymbol{x}}) \left\| \frac{\mathrm{d}\mu(\bar{\boldsymbol{x}})}{\mathrm{d}\mu(\bar{\boldsymbol{p}})} \right\|}_{=:\ \hat{f}(\bar{\boldsymbol{p}})} \mathrm{d}\mu(\bar{\boldsymbol{p}})$$

Material-form reparameterization [Zhang et al. 2020]

Dependent of θ

Difficult to differentiate

Independent of θ

Easier to differentiate

Differential Time-Gated Path Integral

(Material-form) time-gated path integral $I = \int_{\hat{\Omega}} W_\tau(\|\bar{\boldsymbol{x}}\|)\, \hat{f}(\bar{\boldsymbol{p}})\, \mathrm{d}\mu(\bar{\boldsymbol{p}})$

Differentiate

Differential time-gated path integral

$$\frac{\mathrm{d}I}{\mathrm{d}\theta} = \int_{\hat{\Omega}} \frac{\mathrm{d}}{\mathrm{d}\theta}\left[W_\tau(\|\bar{\boldsymbol{x}}\|)\, \hat{f}(\bar{\boldsymbol{p}})\right] \mathrm{d}\mu(\bar{\boldsymbol{p}}) + \int_{\partial\hat{\Omega}} W_\tau(\|\bar{\boldsymbol{x}}\|)\, g(\bar{\boldsymbol{p}})\, \mathrm{d}\dot{\mu}(\bar{\boldsymbol{p}}) + \sum_{s \in \Delta\mathbb{R}[W_\tau]} \int_{\partial\hat{\Omega}_\tau(\|\bar{\boldsymbol{x}}\|)} \Delta W_\tau(s)\, h(\bar{\boldsymbol{p}})\, \mathrm{d}\dot{\mu}_\tau(\bar{\boldsymbol{p}})$$

Interior component

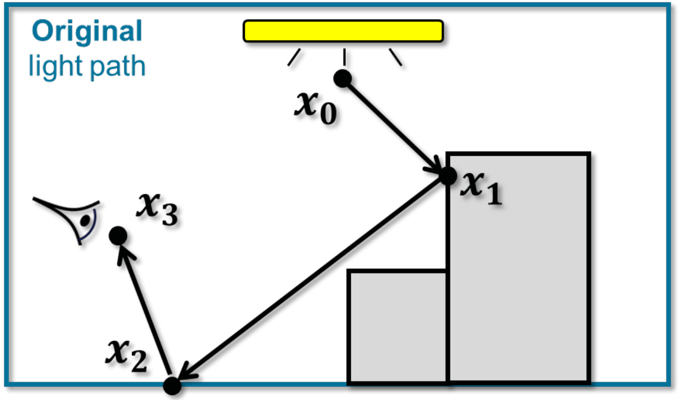

- Differentiated integrand with $W_\tau(\|\bar{\boldsymbol{x}}\|)$

Differential Time-Gated Path Integral

$$\frac{\mathrm{d}I}{\mathrm{d}\theta} = \int_{\hat{\Omega}} \frac{\mathrm{d}}{\mathrm{d}\theta} \left[W_\tau(\|\bar{\boldsymbol{x}}\|) \, \hat{f}(\bar{\boldsymbol{p}}) \right] \mathrm{d}\mu(\bar{\boldsymbol{p}}) + \int_{\partial\hat{\Omega}} W_\tau(\|\bar{\boldsymbol{x}}\|) \, g(\bar{\boldsymbol{p}}) \, \mathrm{d}\dot{\mu}(\bar{\boldsymbol{p}}) + \sum_{s \in \Delta\mathbb{R}[W_\tau]} \int_{\partial\hat{\Omega}_\tau(\|\bar{\boldsymbol{x}}\|)} \Delta W_\tau(s) \, h(\bar{\boldsymbol{p}}) \, \mathrm{d}\dot{\mu}_\tau(\bar{\boldsymbol{p}})$$

- Generalization of the steady-state version (PSDR by Zhang et al. 2020)
- Paths with exactly one **boundary segment**

Visibility boundary component

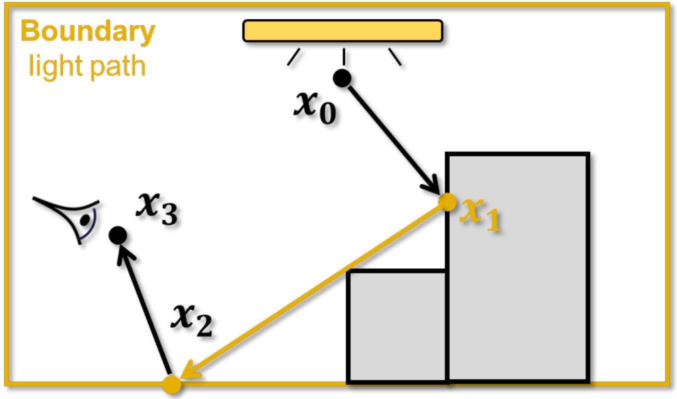

x_1 is on the visibility boundary w.r.t. x_2

Path-Length Boundary Integral

$$\frac{\mathrm{d}I}{\mathrm{d}\theta} = \int_{\hat{\Omega}} \frac{\mathrm{d}}{\mathrm{d}\theta}\left[W_\tau(\|\bar{\boldsymbol{x}}\|)\,\hat{f}(\bar{\boldsymbol{p}})\right]\mathrm{d}\mu(\bar{\boldsymbol{p}}) + \int_{\partial\hat{\Omega}} W_\tau(\|\bar{\boldsymbol{x}}\|)\,g(\bar{\boldsymbol{p}})\,\mathrm{d}\dot{\mu}(\bar{\boldsymbol{p}}) + \sum_{s\in\Delta\mathbb{R}[W_\tau]} \int_{\partial\hat{\Omega}_\tau(\|\bar{\boldsymbol{x}}\|)} \Delta W_\tau(s)\,h(\bar{\boldsymbol{p}})\,\mathrm{d}\dot{\mu}_\tau(\bar{\boldsymbol{p}})$$

- Handle discontinuities in W_τ

  $\Delta\mathbb{R}[W_\tau] = \{\tau_{\min}, \tau_{\max}\}$

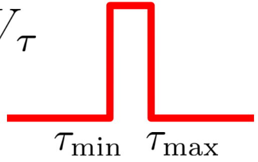

- Unique to diff. time-gated rendering

Path-length boundary component

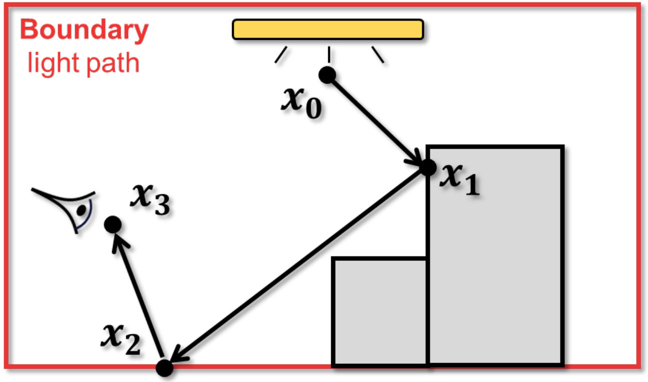

Path length $\|\bar{x}\|$ is a discontinuity point of W_τ

Path-Length Boundary Integral

$$\sum_{s \in \Delta\mathbb{R}[W_\tau]} \int_{\partial\hat{\boldsymbol{\Omega}}_\tau(\|\bar{\boldsymbol{x}}\|)} \Delta W_\tau(s) \underbrace{\hat{f}(\bar{\boldsymbol{p}}) v_\tau(\boldsymbol{q})}_{=:\, h(\bar{\boldsymbol{p}})} \, \mathrm{d}\dot{\mu}_\tau(\bar{\boldsymbol{p}})$$

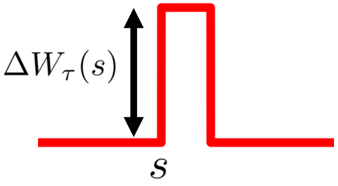

- $\Delta W_\tau(s)$: Difference of path-length importance across the discontinuity boundary
- $\hat{f}(\bar{\boldsymbol{p}})$: Path contribution function
- $v_\tau(\boldsymbol{q})$: Computed from the evolution of path-length boundaries

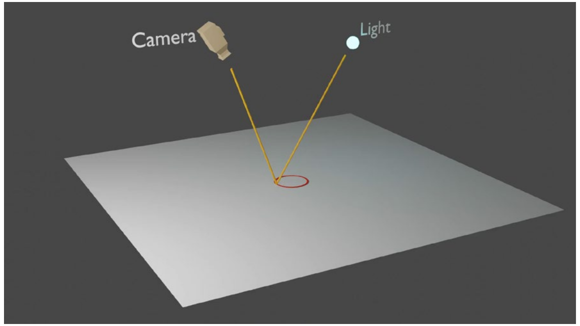

Monte Carlo Estimators

Estimating Interior Integral

$$\frac{\mathrm{d}I}{\mathrm{d}\theta} = \boxed{\int_{\hat{\mathbf{\Omega}}} \frac{\mathrm{d}}{\mathrm{d}\theta}\left[W_\tau(\|\bar{\boldsymbol{x}}\|)\,\hat{f}(\bar{\boldsymbol{p}})\right] \mathrm{d}\mu(\bar{\boldsymbol{p}})} + \int_{\partial\hat{\mathbf{\Omega}}} W_\tau(\|\bar{\boldsymbol{x}}\|)\, g(\bar{\boldsymbol{p}})\, \mathrm{d}\dot{\mu}(\bar{\boldsymbol{p}}) + \sum_{s\in\Delta\mathbb{R}[W_\tau]} \int_{\partial\hat{\mathbf{\Omega}}_\tau(\|\bar{\boldsymbol{x}}\|)} \Delta W_\tau(s)\, h(\bar{\boldsymbol{p}})\, \mathrm{d}\dot{\mu}_\tau(\bar{\boldsymbol{p}})$$

- Sample a path using standard methods (unidirectional PT)
- Incorporate path-length importance

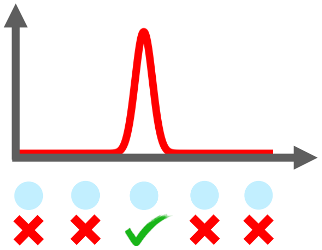

Narrow time gate → **Few** paths contribute to the integral

Handling Narrow Time Gate

- Ellipsoidal next-event estimation
  - Step 1: Sample a path length
    $\tau_0 \sim W_\tau(\|\bar{\boldsymbol{x}}\|)$
  - Step 2: Trace a path from camera and sample a point on light
  - Step 3: Ellipsoidal connection [Pediredla et al. 2019]

$\boldsymbol{q}$ is on an ellipsoid such that
$\|\boldsymbol{p}_0 - \boldsymbol{q}\| + \|\boldsymbol{q} - \boldsymbol{p}_1\| = \tau_0 - \|\boldsymbol{p}_1 - \boldsymbol{p}_2\|$

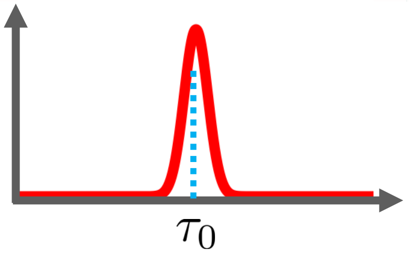

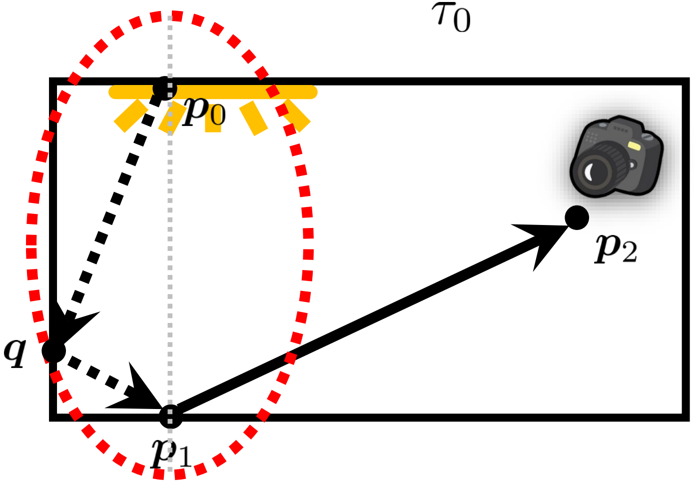

Handling Narrow Time Gate

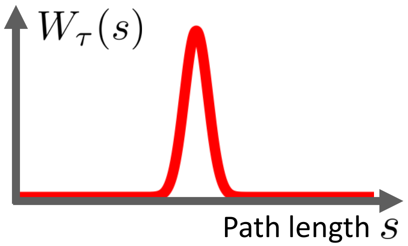

Near-delta Gaussian

Differentiate w.r.t. s

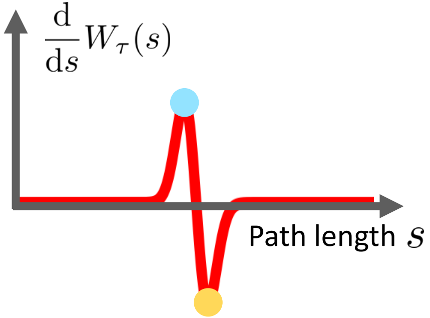

High-magnitude positive value and negative value

High variance!

- Antithetic sampling [Zhang et al. 2021]
  - Generate a pair of negatively correlated samples
  - High-magnitude derivatives cancel out

$$\frac{\mathrm{d}}{\mathrm{d}s}W_\tau(\bullet) + \frac{\mathrm{d}}{\mathrm{d}s}W_\tau(\bullet) = 0$$

Handling Narrow Time Gate

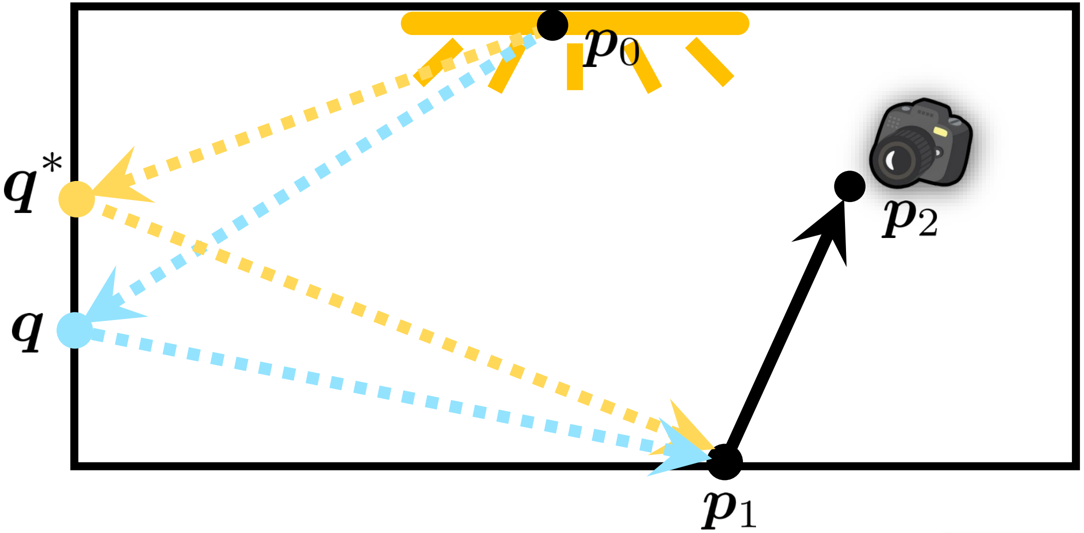

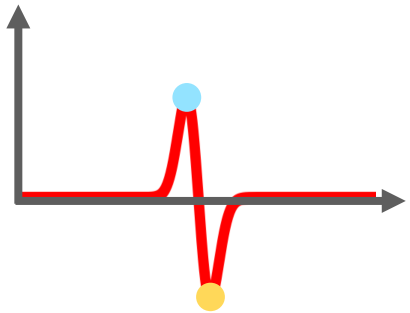

Construct two correlated paths

$\|\bar{x}\| =$ (blue) $\|\bar{x}^*\| =$ (yellow)

$$\frac{\mathrm{d}}{\mathrm{d}\theta} W_\tau(\|\bar{x}\|) + \frac{\mathrm{d}}{\mathrm{d}\theta} W_\tau(\|\bar{x}^*\|) \approx 0$$

Contributions largely cancel out

Evaluation

Estimating Interior Integral

- Configuration: near-delta time gate, derivative w.r.t. the vertical position

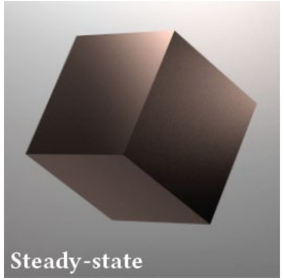

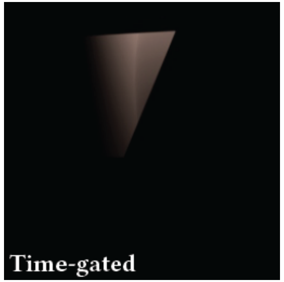

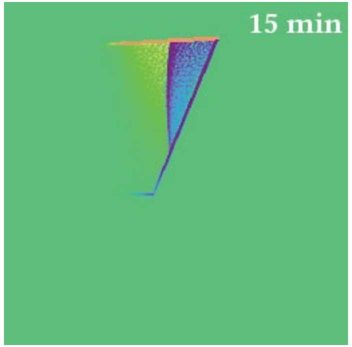

Reference of interior integral

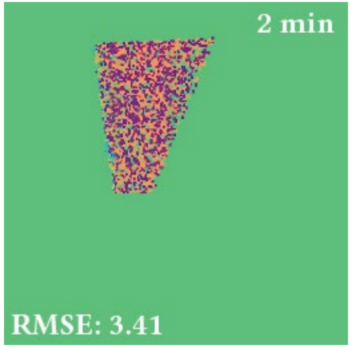

Standard estimator

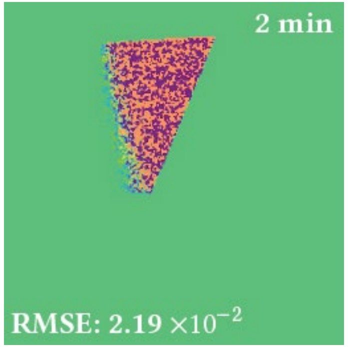

Ellipsoidal NEE

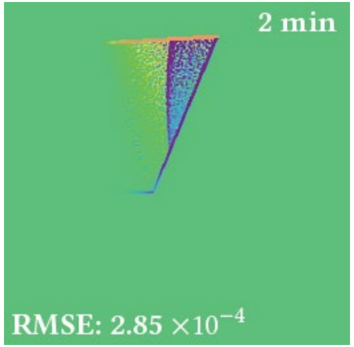

Ellipsoidal NEE + antithetic

Estimating Visibility Boundary

$$\frac{\mathrm{d}I}{\mathrm{d}\theta} = \int_{\hat{\Omega}} \frac{\mathrm{d}}{\mathrm{d}\theta}\left[W_\tau(\|\bar{\boldsymbol{x}}\|)\,\hat{f}(\bar{\boldsymbol{p}})\right]\mathrm{d}\mu(\bar{\boldsymbol{p}}) + \boxed{\int_{\partial\hat{\Omega}} W_\tau(\|\bar{\boldsymbol{x}}\|)\,g(\bar{\boldsymbol{p}})\,\mathrm{d}\dot{\mu}(\bar{\boldsymbol{p}})} + \sum_{s\in\Delta\mathbb{R}[W_\tau]} \int_{\partial\hat{\Omega}_\tau(\|\bar{\boldsymbol{x}}\|)} \Delta W_\tau(s)\,h(\bar{\boldsymbol{p}})\,\mathrm{d}\dot{\mu}_\tau(\bar{\boldsymbol{p}})$$

- Multi-directional sampling [Zhang et al. 2020]
- Using ellipsoidal NEE if time gate is narrow

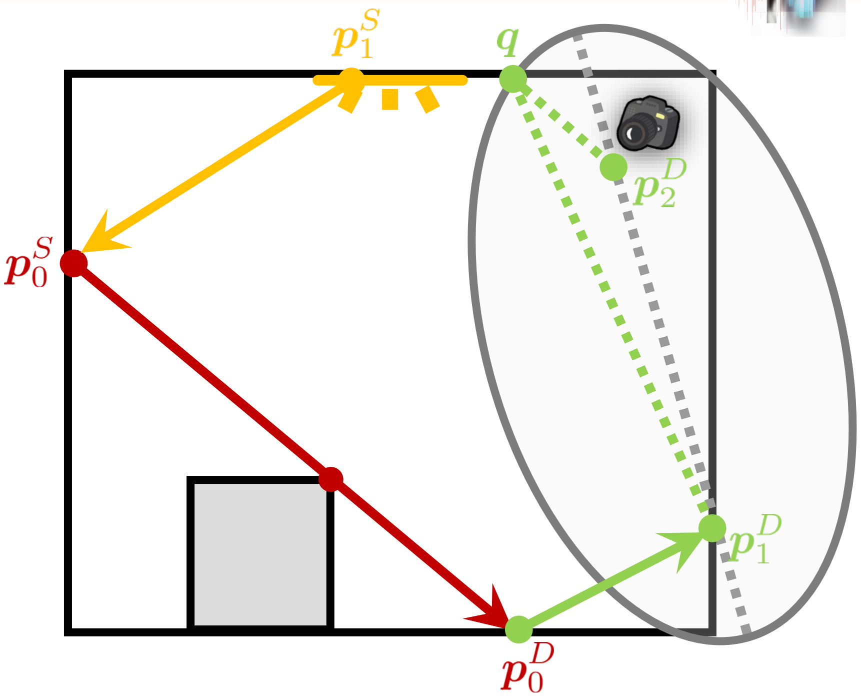

Estimating Path-Length Boundary

$$\frac{\mathrm{d}I}{\mathrm{d}\theta} = \int_{\hat{\Omega}} \frac{\mathrm{d}}{\mathrm{d}\theta}\left[W_\tau(\|\bar{\boldsymbol{x}}\|)\,\hat{f}(\bar{\boldsymbol{p}})\right]\mathrm{d}\mu(\bar{\boldsymbol{p}}) + \int_{\partial\hat{\Omega}} W_\tau(\|\bar{\boldsymbol{x}}\|)\,g(\bar{\boldsymbol{p}})\,\mathrm{d}\dot{\mu}(\bar{\boldsymbol{p}}) + \sum_{s\in\Delta\mathbb{R}[W_\tau]}\int_{\partial\hat{\Omega}_\tau(\|\bar{\boldsymbol{x}}\|)} \Delta W_\tau(s)\,h(\bar{\boldsymbol{p}})\,\mathrm{d}\dot{\mu}_\tau(\bar{\boldsymbol{p}})$$

- **Ellipsoidal NEE** is mandatory
- **Antithetic sampling** for variance reduction

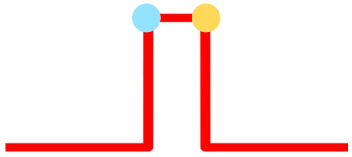

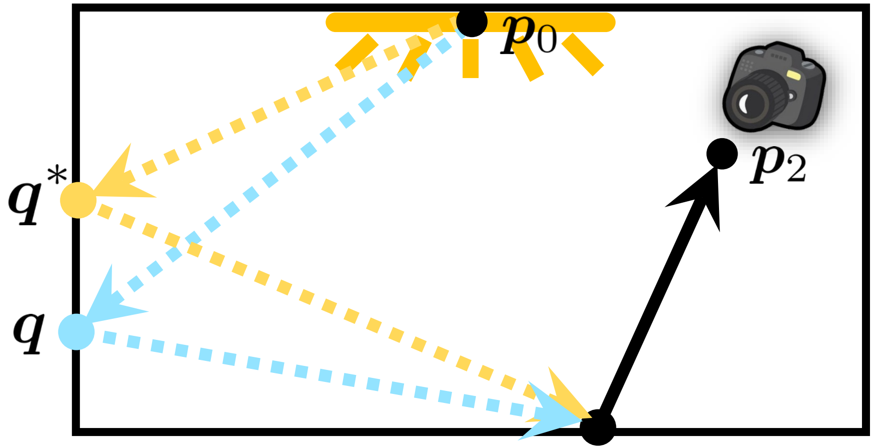

Evaluation

Estimating Path-Length Boundary Integral

- Configuration: near-delta time gate, derivative w.r.t. the vertical position

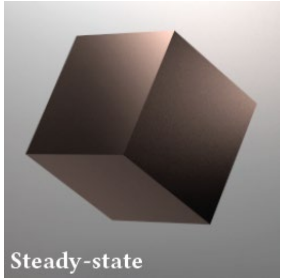

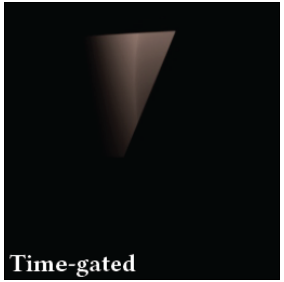

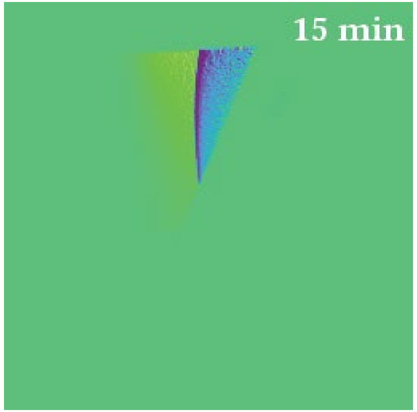

Reference of path-length boundary

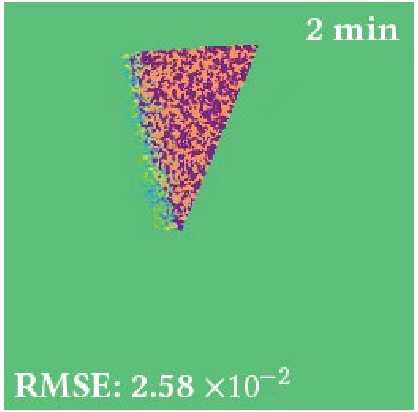

Ellipsoidal NEE

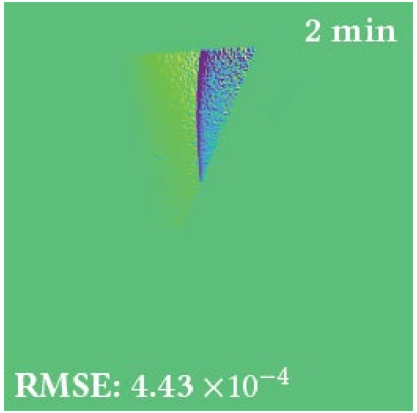

Ellipsoidal NEE + antithetic

Results

Validation

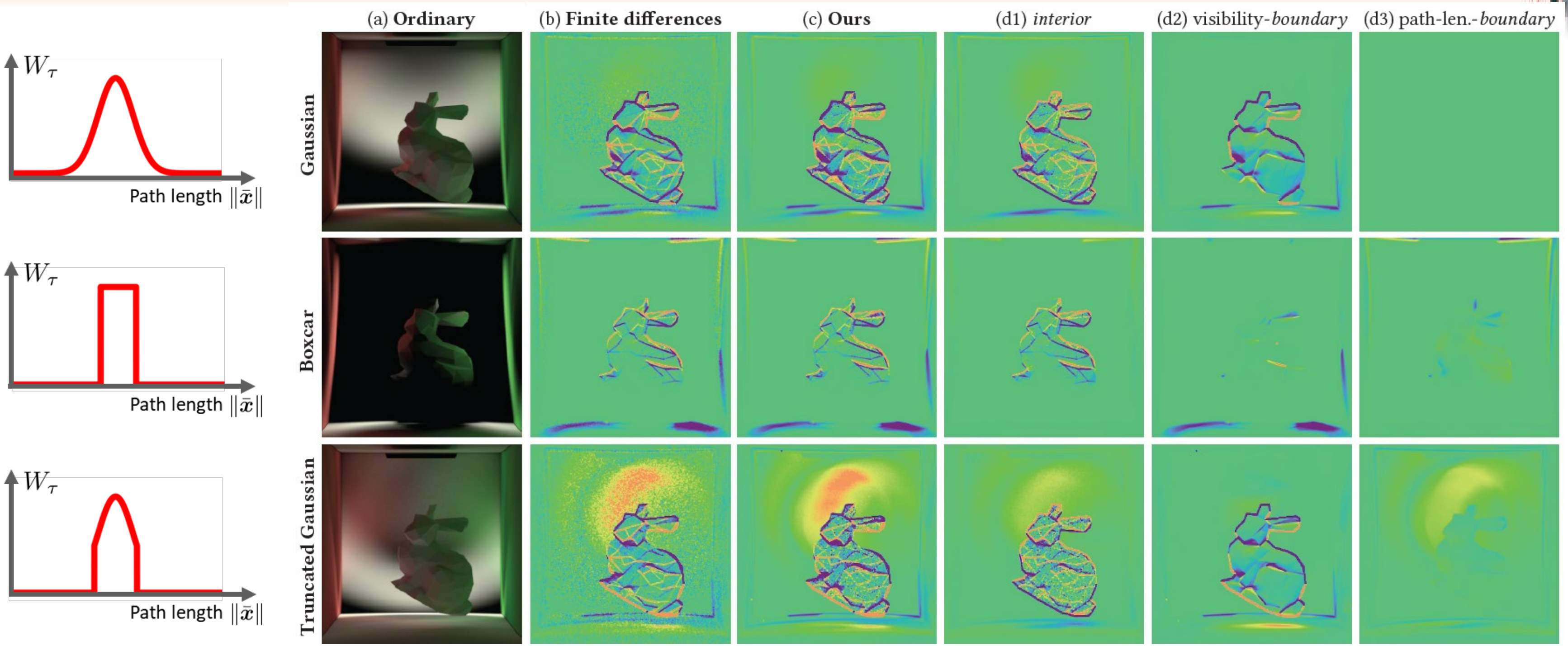

W_τ
Path length $\|\bar{x}\|$
W_τ
Path length $\|\bar{x}\|$
W_τ
Path length $\|\bar{x}\|$
(a) **Ordinary**
(b) **Finite differences**
(c) **Ours**
(d1) *interior*
(d2) visibility-*boundary*
(d3) path-len.-*boundary*
Gaussian
Boxcar
Truncated Gaussian

Inverse Rendering Results

Bunny

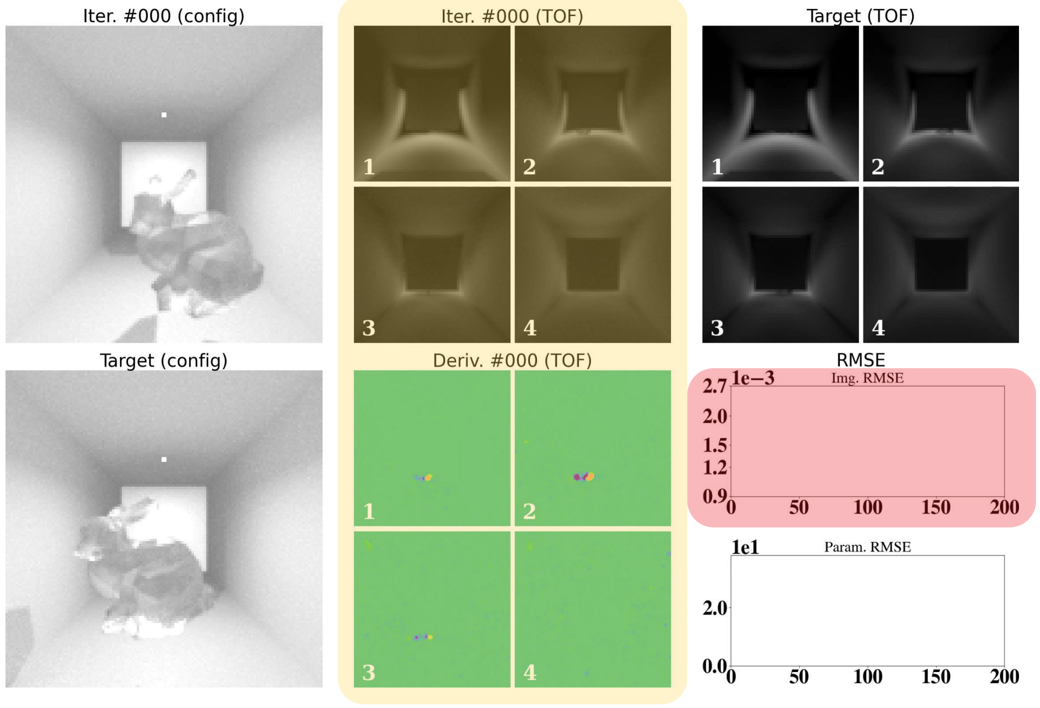

- A rough-glass bunny inside a diffuse box
- ToF camera is **blocked** (NLOS configuration)
- Search for position
- 20 ToF images used, 4 shown
- Only the **image loss** is used for optimization

Inverse Rendering Results

Tree

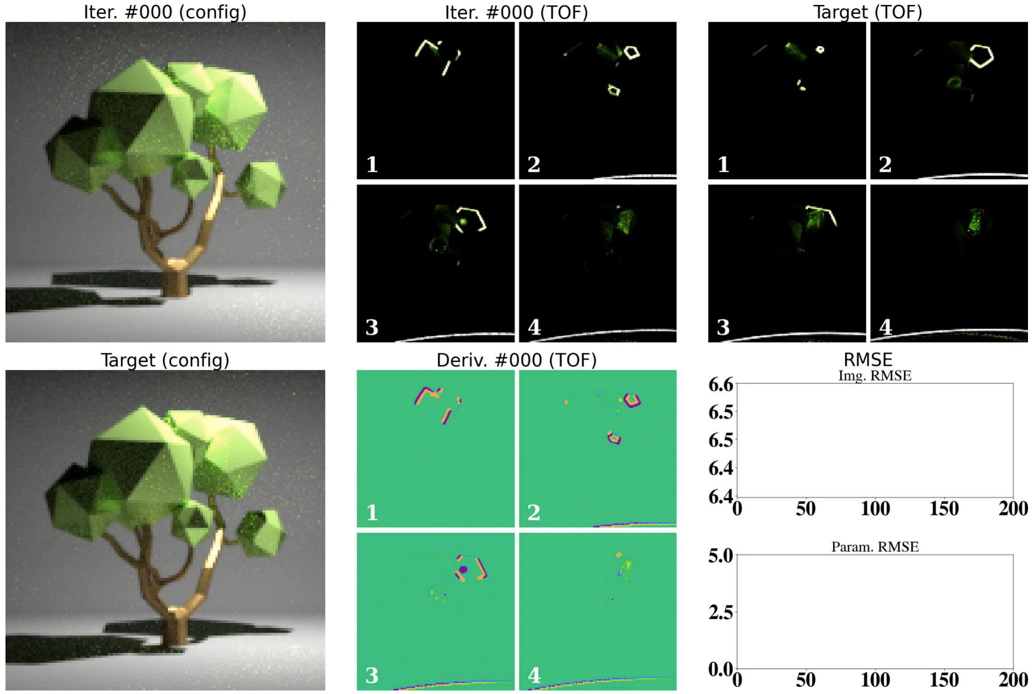

- A glossy tree model lit by a small area light
- Search for the **position** of the light source
- Near-delta time gate

Inverse Rendering Results

Height field (ToF)

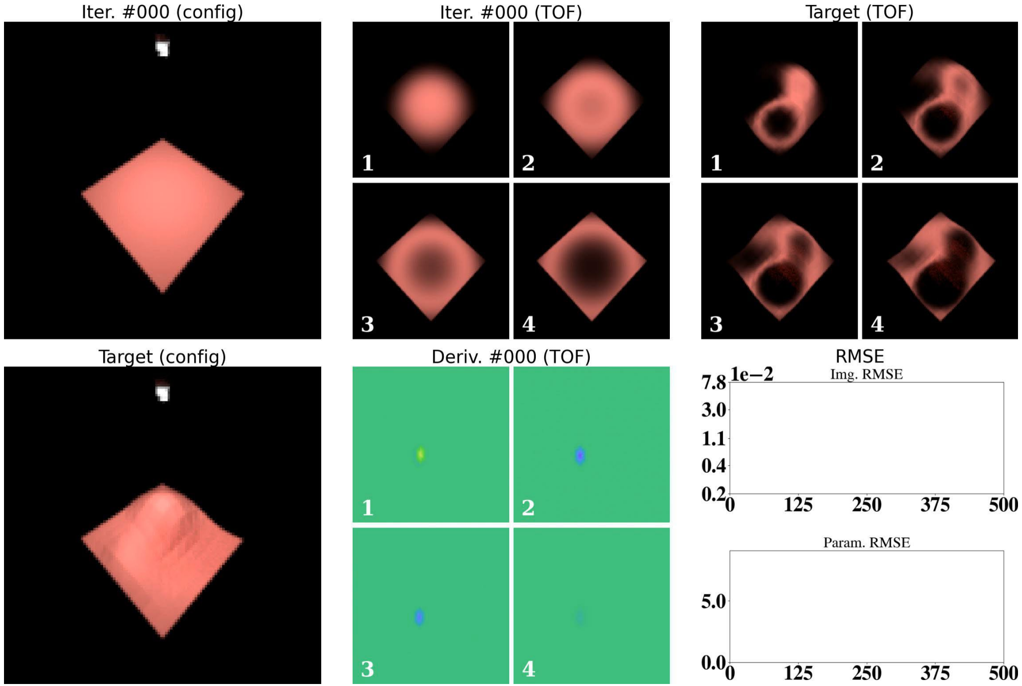

- Search for the height of each vertex (121 unknown variables)
- 12 ToF images used, 4 shown

Converged

Inverse Rendering Results

Height field (steady-state)

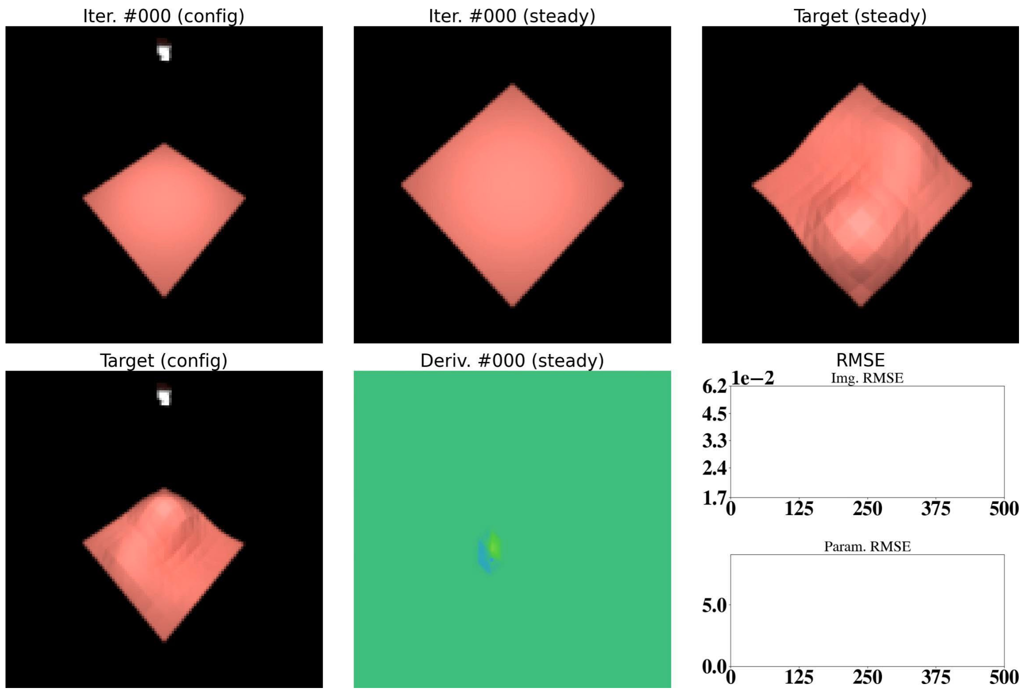

- A single steady-state image is used
- Optimization becomes highly under-constrained

Get stuck at a local minimum

Inverse Rendering Results

Corridor (Full interreflections, our estimator)

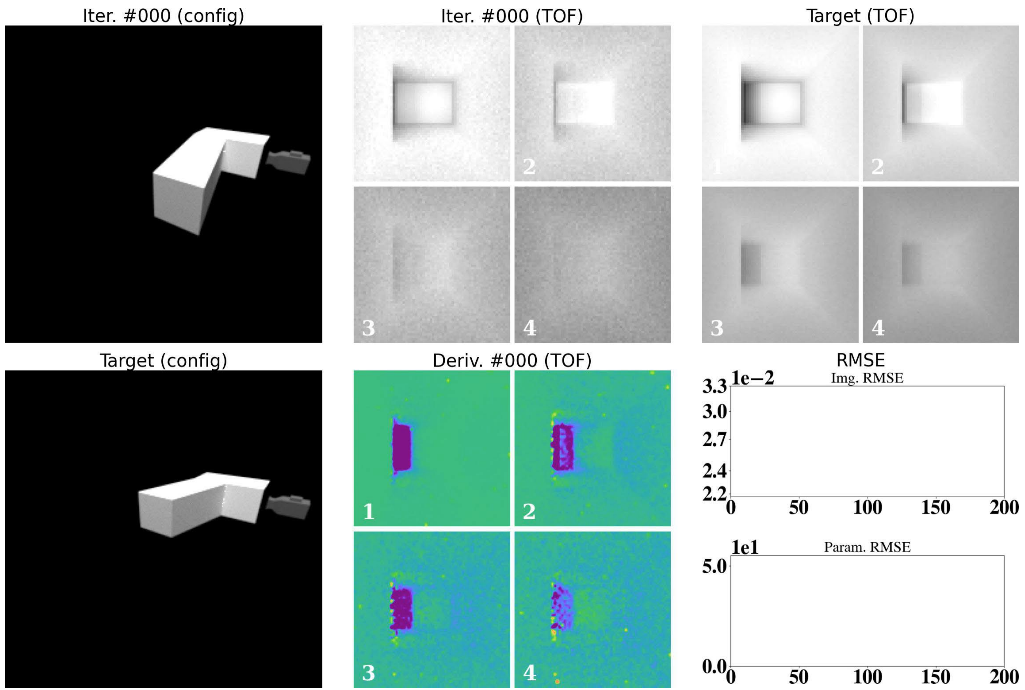

- Search for the position of the end of the corridor
- Not directly visible to the camera (NLOS)
- Concave shape
- Simulating **full inter-reflections** is crucial

Inverse Rendering Results
Corridor (3 bounces)

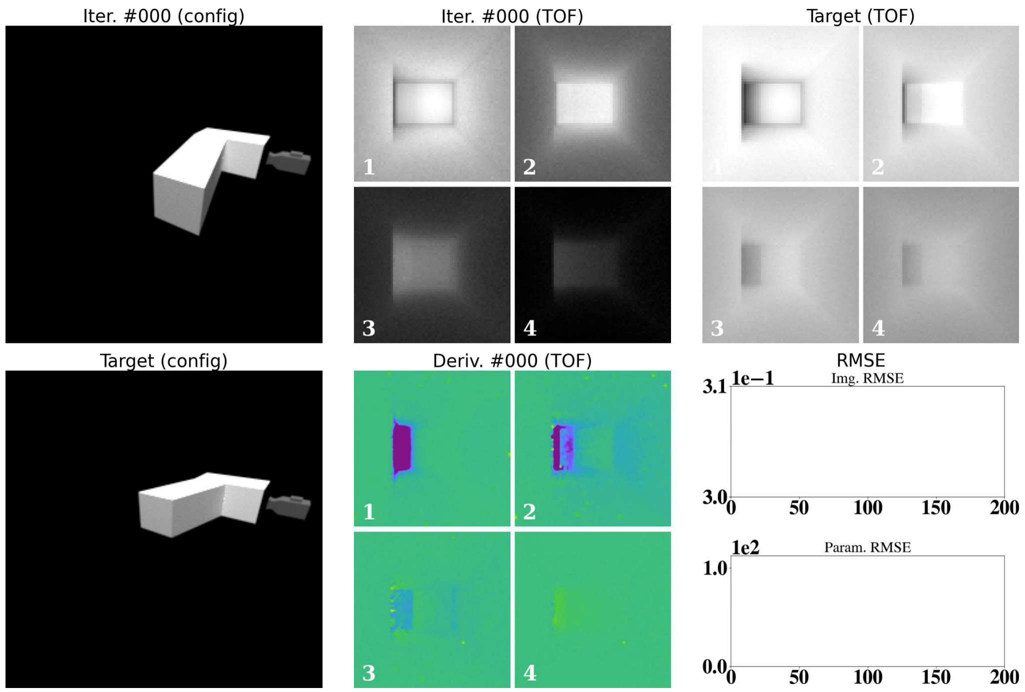

- Simulating **only 3 bounces**
- Suffering significant energy loss

Diverge

Inverse Rendering Results

Corridor (Full interreflections, finite differences)

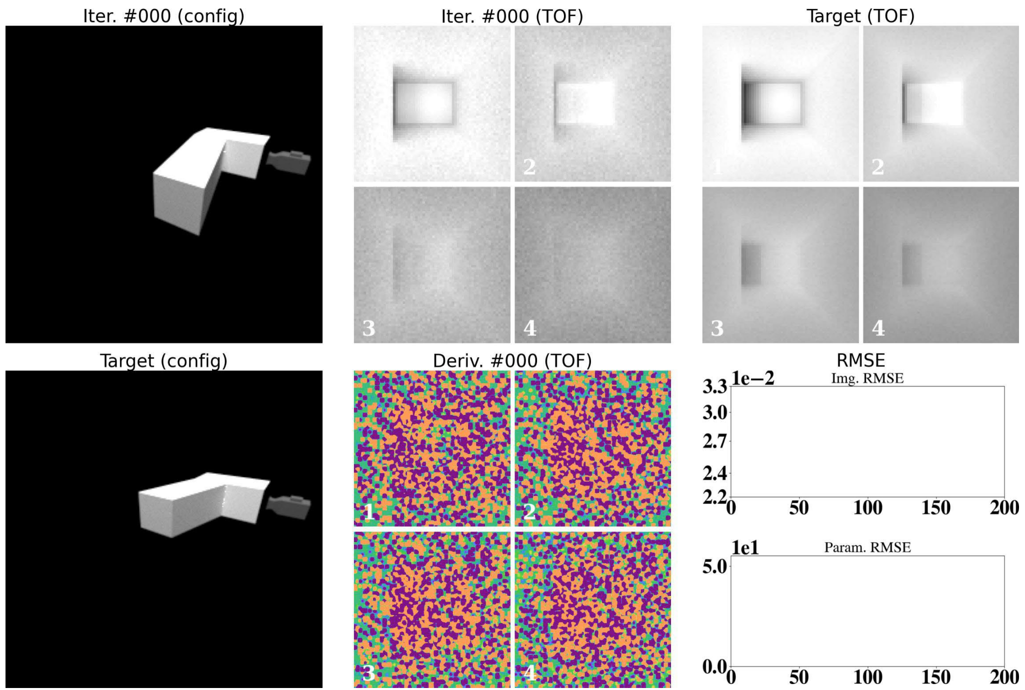

- Derivatives computed using **finite differences**
- Derivative estimates are biased and high-variance

Fail to converge

Limitations and Future Work

- Volumetric light transport
- Dirac delta path-length importance function
  - Interior integral involves 2^{nd}-order derivatives
- Current implementation: CPU-based, simple forward-mode autodiff
  - GPU-based system [Nimier-David et al. 2019, 2020; Vicini et al. 2021]
  - Ability to handle millions of parameters
  - Real-world large-scale ToF imaging problems

Conclusion

- Differential time-gated path integral

$$\frac{\mathrm{d}I}{\mathrm{d}\theta} = \int_{\hat{\Omega}} \frac{\mathrm{d}}{\mathrm{d}\theta}\left[W_\tau(\|\bar{\boldsymbol{x}}\|)\,\hat{f}(\bar{\boldsymbol{p}})\right]\mathrm{d}\mu(\bar{\boldsymbol{p}}) + \int_{\partial\hat{\Omega}} W_\tau(\|\bar{\boldsymbol{x}}\|)\,g(\bar{\boldsymbol{p}})\,\mathrm{d}\dot{\mu}(\bar{\boldsymbol{p}}) + \boxed{\sum_{s\in\Delta\mathbb{R}[W_\tau]} \int_{\partial\hat{\Omega}_\tau(\|\bar{\boldsymbol{x}}\|)} \Delta W_\tau(s)\,h(\bar{\boldsymbol{p}})\,\mathrm{d}\dot{\mu}_\tau(\bar{\boldsymbol{p}})}$$

Unique path-length boundary caused by

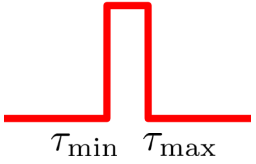

- Efficient Monte Carlo estimators
  - Ellipsoidal NEE

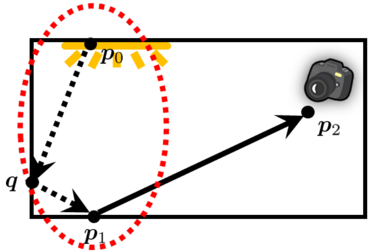

  - Antithetic sampling

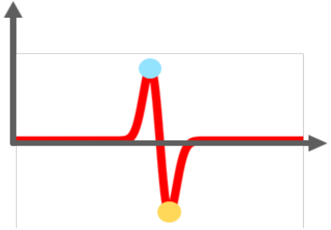

Acknowledgements

- Anonymous reviewers
- Funding: NSF 1900927, NSF 2105806, NVIDIA Graduate Fellowship, the Ronald L. Graham Chair

Project webpage
https://bit.ly/3vIn2jn

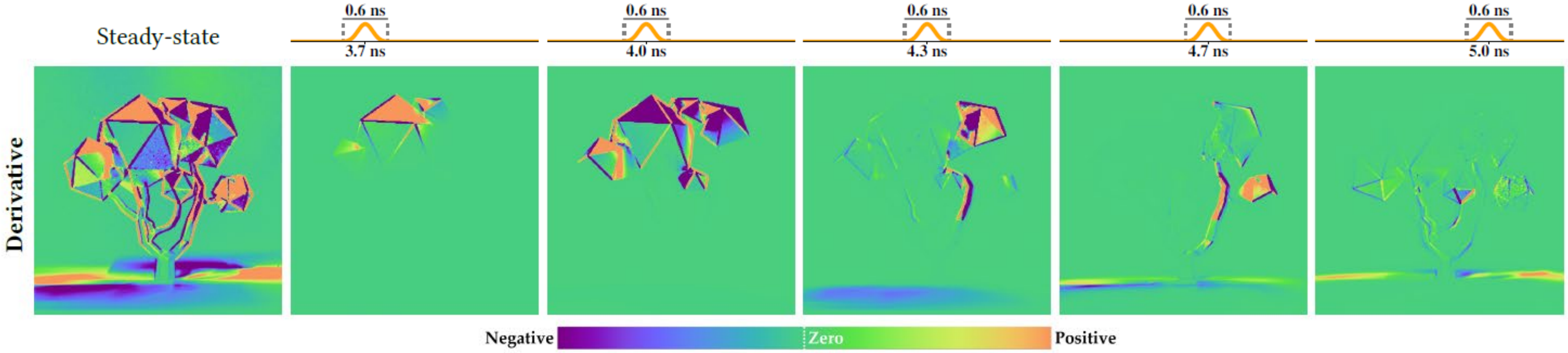

SIGGRAPH ASIA 2021 TOKYO

CONFERENCE 14 - 17 DECEMBER 2021
EXHIBITION 15 - 17 DECEMBER 2021
TOKYO INTERNATIONAL FORUM, JAPAN

sa2021.siggraph.org

LIVE

Thank you for your attention!

Sponsored by

acm

Organized by

koelnmesse
we energize your business | since 1924